

Induction of Fibroblast-to-Myofibroblast Differentiation by Changing Cytoplasmic Actin Ratio

Yulia G. Levuschkina^{1,2#}, Vera B. Dugina^{1,2#}, Galina S. Shagieva¹,
Sergey V. Boichuk^{3,4}, Ilya I. Eremin⁵, Natalia V. Khromova⁶, and Pavel B. Kopnin^{6,a*}

¹Belozersky Research Institute of Physico-Chemical Biology,
Lomonosov Moscow State University, 119992 Moscow, Russia

²Faculty of Biology, Lomonosov Moscow State University, 119991 Moscow, Russia

³Department of Pathology, Kazan State Medical University, 420012 Kazan, Russia

⁴Department of Radiotherapy and Radiology,
Russian Medical Academy of Continuous Professional Education, 119454 Moscow, Russia

⁵Petrovsky National Research Center of Surgery, 119991 Moscow, Russia

⁶Scientific Research Institute of Carcinogenesis,
N. N. Blokhin National Medical Research Center of Oncology, 115478 Moscow, Russia

^ae-mail: pbkopnin@mail.ru

Received November 19, 2024

Revised January 9, 2025

Accepted January 14, 2025

Abstract—Myofibroblasts, which play a crucial role in the tumour microenvironment, represent a promising avenue for research in the field of oncotherapy. This study investigates the potential for the induced differentiation of human fibroblasts into myofibroblasts through downregulation of the γ -cytoplasmic actin (γ -CYA) achieved by RNA interference. A decrease in the γ -CYA expression in human subcutaneous fibroblasts resulted in upregulation of myofibroblast markers, including α -smooth muscle actin (α -SMA), ED-A FN, and type III collagen. These changes were accompanied by notable alterations in cellular morphology, characterized by a significant increase in cell area and the formation of pronounced supermature focal adhesions. Downregulation of γ -CYA resulted in the compensatory increase in expression of the β -cytoplasmic actin and α -SMA, and formation of the characteristic α -SMA-positive stress fibers. In conclusion, our results demonstrate that a decrease in the γ -CYA expression leads to myofibroblastic trans-differentiation of human subcutaneous fibroblasts.

DOI: 10.1134/S000629792460412X

Keywords: actin isoforms, fibroblasts, myofibroblasts, stromal microenvironment, differentiation

INTRODUCTION

Actin is represented by six different isoforms in higher vertebrates, two of which, β - and γ -cytoplasmic actins (β -CYA and γ -CYA), are ubiquitously expressed in all cell types. The ratio of these two isoforms has been demonstrated to influence phenotypic

properties and functional activities of the cells [1]. The study of intracellular localization and functional roles of β -CYA and γ -CYA became feasible following development of monoclonal antibodies highly specific to γ -CYA. The use of polyclonal antibodies is limited due to the potential for cross-reactivity between γ -CYA and α -smooth muscle actin (α -SMA) [2]. Researchers

Abbreviations: α -SMA, α -smooth muscle actin; β -CYA, β -cytoplasmic actin; γ -CYA, γ -cytoplasmic actin; CAMs, cancer-associated myofibroblasts; ECM, extracellular matrix; ED-A FN, fibronectin extra domain A; FAs, focal adhesions; IF, immunofluorescence; shRNA, short hairpin RNA; SMM, smooth muscle myosin.

* To whom correspondence should be addressed.

These authors contributed equally to this study.

have attempted to determine the role of cytoplasmic actin isoforms by selectively inhibiting expression of each using short hairpin RNA (shRNA). Decrease of the β -CYA expression in fibroblasts led to an increase in cell surface area, formation of multiple protrusions, and disassembly of stress fibers, while the downregulation of γ -CYA resulted in the acquisition of a “contractile phenotype” with well-defined actin bundles [2, 3]. Furthermore, fibroblasts with reduced expression of β -CYA or γ -CYA exhibited distinctive patterns of cell motility in comparison with the control cell culture, indicating that both cytoplasmic actin isoforms could have a specific role in regulating cell motility [2, 4].

Since their initial identification, myofibroblasts attracted significant attention within the scientific community, having been implicated in a multitude of pathological processes, including those associated with tumour progression. The designation “cancer-associated myofibroblasts” (CAMs) is frequently used to describe this specific type of myofibroblasts. The role of CAMs in tumour progression is complex and multifaceted. In particular, myofibroblasts initially exert an anti-tumour effect, but subsequently become activated by factors secreted by the tumour and contribute to its growth and progression [5]. CAMs are the primary source of extracellular matrix (ECM) components that facilitate tumour cell growth and progression. These include matricellular proteins such as connective tissue growth factor (CTGF), tenascin C, fibronectin, collagens, and elastin [6].

Myofibroblasts associated with tumour stroma can be activated from different progenitor cells. Under normal conditions, progenitor cells in the intact tissue are protected by an extracellular matrix of a specific composition, which prevents development of enhanced contractile properties. In the event of a disruption of tissue homeostasis, the release of inflammatory signals activates stromal cells to remodel ECM. This results in a gradual increase of stiffness, thereby facilitating formation of contractile bundles of microfilaments, which are known as stress fibers. This phase is characterized by generation of protomyofibroblasts. Subsequently, transforming growth factor (most often TGF β 1), which is a chemical factor, in combination with a rigid ECM, which is a mechanical factor, stimulates expression of α -SMA by protomyofibroblasts and incorporation of this actin isoform into stress fibers. This results in further remodelling of ECM. The combination of physicochemical factors originating from protomyofibroblasts and differentiated myofibroblasts facilitates epithelial cell transformation and tumour progression [6, 7].

The primary marker of myofibroblasts at the present time is α -smooth muscle actin (α -SMA) isoform, which has been identified in stress fibers with distinctive contractile properties [5]. Protomyofibro-

blasts are distinguished by the formation of stress fibers composed of β -CYA [8].

Clarification of myofibroblast cytogenesis is inextricably linked to the challenge of their identification. These cells could be distinguished from fibroblasts by their capacity for contraction, presence of organized bundles of microfilaments, and their interaction with matrix and other cells. However, similar cell types, such as smooth muscle cells (SMC), could also exhibit similar functional properties and, therefore, be considered to align with this description [9].

Hence, the necessity for identification of particular molecular markers that can be used to distinguish between the closely related cell types is evident. The initial assumption that α -smooth muscle actin is an optimal molecular marker for this purpose, which is based on the fibroblast-myofibroblast differentiation pathway, is ambivalent in the case when SMC or myoepithelial cells are present in close proximity to putative myofibroblasts [10]. Furthermore, studies have indicated the potential for interchangeability between the different actin isoforms. Nevertheless, this does not imply that α -smooth muscle actin should be discarded as a marker for identification purposes [11]. It is sufficient to introduce additional parameters to enhance accuracy of identification.

In the present study, we investigated the potential of fibroblast differentiation into myofibroblasts, with the objective of elucidating the role of the cytoplasmic actin ratio in this process. Using the previously created lentiviral genetically engineered constructs with proven efficacy [12, 13], we partially or completely downregulated γ -CYA and performed comparative morphometric analyses with the control at different time points. Efficiency of the γ -CYA downregulation was evaluated through the determination of the quantity of mRNA using classical PCR analysis, measurement of the amount of protein (immunoblotting), as well as observation of morphological alterations and calculation of the percentage of cells exhibiting downregulation of γ -CYA (phase-contrast and immunofluorescence microscopy).

MATERIALS AND METHODS

Cell culture. Fibroblast cell cultures were acquired from the culture collection of the cytogenetics laboratory of the Scientific Research Institute of Carcinogenesis, N. N. Blokhin National Medical Research Center of Oncology. The cells were cultivated in a DMEM-HiGluc medium with Glutamax (glutamine was present in the medium) and NEAA (a mixture of essential amino acids).

RNA interference. The most efficient 21-bp sequence was selected for shRNA expression and

inhibition of γ -CYA mRNA at position 1790-1811: 5'-CAGCAACACACACGTCATTGTGTGTAA-3'. The corresponding constructs were synthesized and cloned into the lentiviral vector pLKO.1-puro (Addgene, USA; Plasmid #10878). A control was also included in the form of the pLKO.1-shGFP-puro construct containing a shRNA sequence targeting eGFP (GenBank pEGFP accession number U55761) was used as a control. Oligonucleotide synthesis and DNA sequencing were conducted by Evrogen.

The lentiviral DNA constructs pLKO.1, along with the packaging plasmids p Δ R8.2 (#12263, Addgene) and pVSV-G (#8454, Addgene), were transfected into 293FT packaging cells (R70007, Thermo Fisher Scientific, USA) using TurboFect transfection reagent (R0531, Thermo Fisher Scientific).

Supernatants containing the virus were collected after 1-2 days of incubation and used to infect fibroblasts in the presence of polybrene (8 μ g/ml, Sigma-Aldrich, USA). The infected cell cultures were maintained for 4-5 days in a medium containing 1 μ g/ml puromycin (Sigma-Aldrich). The cells were used in experiments 5-9 days after the onset of infection.

Antibodies. The following primary antibodies were used: mouse monoclonal antibodies – anti- α -SM1 (1A4, IgG2a, AbD Serotec, UK), anti- γ -CYA (2A3, IgG2b, AbD Serotec), anti- β -CYA (4C2, IgG1, AbD Serotec), anti-pan-actin (clone C4, Cell Signaling Technology, USA), anti-paxillin (IgG1, BD Transduction Laboratories, USA), anti-desmin (BD Transduction Laboratories); rabbit monoclonal antibodies – anti-collagen I, anti-elastin and anti-collagen III (AbD Serotec); rabbit polyclonal antibodies – anti-SMM (smooth muscle myosin) antibody (Biorad). Fibronectin extra domain A (ED-A FN) was stained with the IST-9, mouse monoclonal antibody IgG1 specific to the type III domain (kindly provided by Dr. L. Zardi, National Institute for Cancer Research, Laboratory of Cell Biology, Genoa, Italy).

The following secondary antibodies were employed: goat anti-mouse IgG H&L (Alexa Fluor® 488, Subclass 1/Subclass 2b), goat anti-mouse IgG H&L (Alexa Fluor® 594, Subclass 2b), donkey anti-rabbit IgG H&L (Alexa Fluor® 488), Rhodamine Red™-X-conjugated donkey anti-mouse IgG H&L (Jackson ImmunoResearch Laboratories, UK). DAPI (D9542, Sigma-Aldrich) was used for nuclear staining during incubation with the secondary antibodies. For the purpose of Western blot analysis, HRP-conjugated secondary antibodies were used, namely anti-mouse IgG and anti-rabbit IgG (Santa Cruz Biotechnology, USA).

Western blot analysis. Cell cultures were lysed on plastic dishes in a RIPA buffer (50 mM Tris-HCl pH 7.4, 150 mM NaCl, 1% Na deoxycholate, 1% NP-40, 0.1% SDS, 100 mM PMSF, 1 mM pepstatin A and 1 mM E64) at 4°C to obtain extracts. Protein concen-

tration in cell lysates was measured using the Bradford assay. Protein samples containing from 5 to 20 μ g were separated in an 8-12% polyacrylamide gel with SDS and transferred to a PVDF membrane (IPFL00010, Millipore).

Membranes were blocked with a SuperBlock Blocking Buffer (Thermo Fisher Scientific) for 15-20 min at room temperature and next stained with specific antibodies for 1 h at room temperature. The membranes were then washed three times for 5 min each with ice-cold PBS with Tween20 (PBS-T) on a shaker. Secondary antibodies were next added and incubated with the membranes followed by another PBS-T wash three times for 5 min each with ice-cold PBS-T. Finally, after pre-drying, the bands were visualized using enhanced chemiluminescence WesternBright Quantum detection kit (Advantra, USA). Densitometric analysis of Western blotting images was performed using TotalLab software (version 1.11) and normalized to total actin levels. Protein levels were estimated by analyzing the results of at least three independent experiments.

Fluorescent immunohistochemistry and immunofluorescent microscopy. For cell fixation, 2% paraformaldehyde was used in a serum-free culture medium with addition of HEPES (1 ml of 1 M HEPES was added per 50 ml of serum-free medium). The fixation period was between eight and ten minutes. Subsequently, the cells on coverslips were subjected to an extraction-fixation process with cold methanol (1 ml per well of a six-well plate) at -20°C for a period of five minutes. Following washing, the cells were stained with antibodies in order to detect cytoskeletal structures in accordance with the established protocols. Immunofluorescence examinations were conducted using a Zeiss Axioplan microscope, equipped with an Olympus DP70 video camera. Two objectives were employed: a 40 \times /0.75 PlanNeofluar and a PlanNeofluar 100 \times /1.3.

Morphometrical and statistical analyses. ImageJ Fiji v1.53u software was used for tracing outlines of the cell, measurement of the cell area, and mean of IF intensity of cytoskeletal proteins per cell. The data were then subjected to further processing with Adobe Photoshop Version: 22.4.2 (2021). The results are presented as a mean \pm standard error of the mean obtained from at least three independent experiments. The results were subjected to statistical evaluation using the Mann-Whitney U-test. Values of $p < 0.001$ (***), $p < 0.01$ (**) and $p < 0.05$ (*) were considered to be statistically significant.

Three square areas with dimensions of 10 \times 10 μ m (100 μ m²) in the lamellar zone of each cell edge, corresponding to locations of the highest total fluorescence of focal adhesions (FAs), were selected for measurement of intensity values. As our objective was to examine changes in the morphometric parameters of

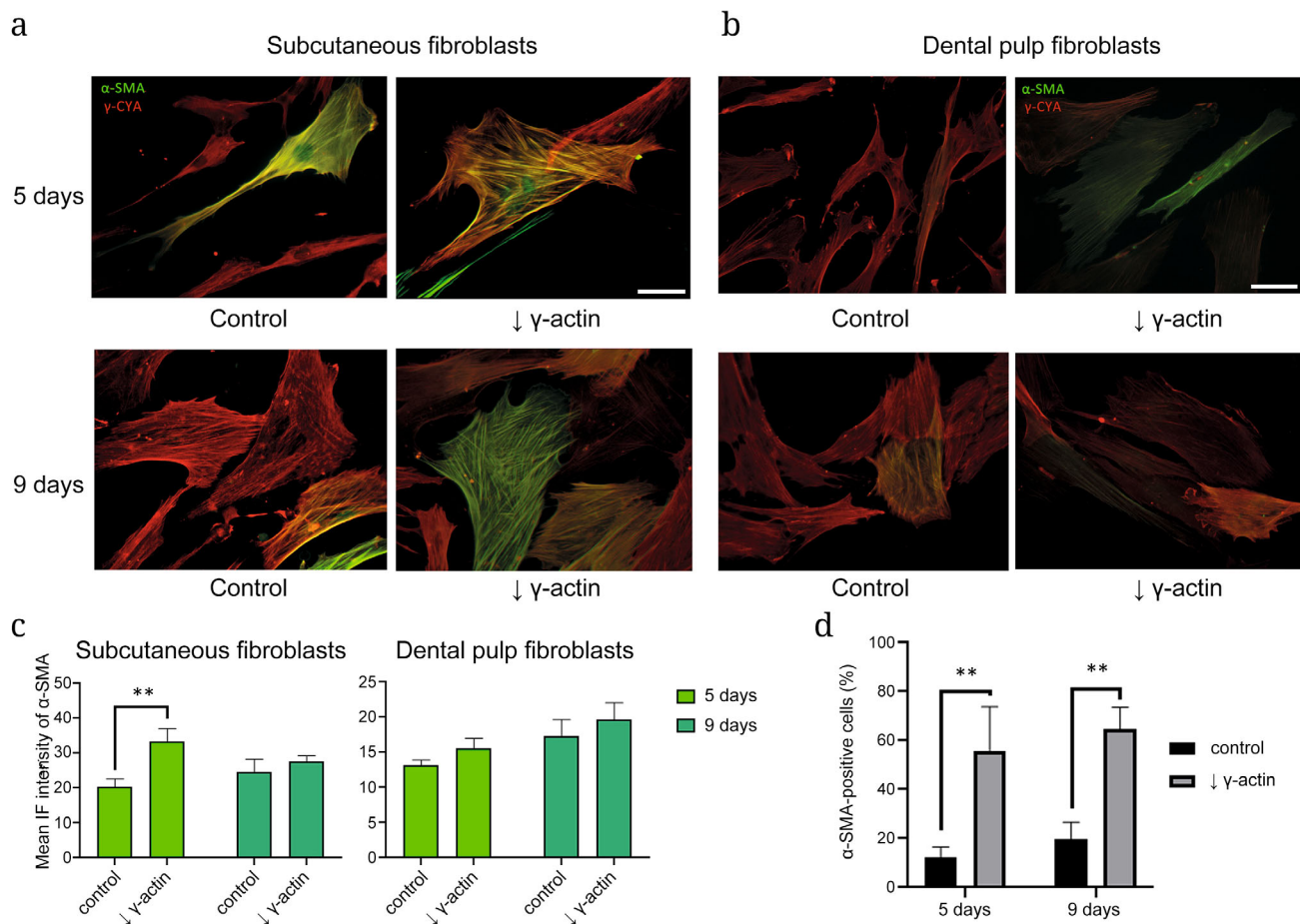


Fig. 1. Cultures of subcutaneous fibroblasts (a) and dental pulp fibroblasts (b) 5 days and 9 days after infection with lentiviral constructs, IF staining for α -SMA (green) and γ -CYA (red). Scale bar is 50 μ m. c) IF intensity of α -SMA in the α -SMA-positive cells in subcutaneous (left) and dental pulp (right) fibroblasts. Graphs show mean \pm SEM. d) Amount of α -SMA-positive cells in the subcutaneous fibroblast cultures in the control and in the cells with downregulated γ -CYA, 5 days and 9 days after infection. Graphs show mean \pm SEM, the mean was calculated based on a minimum of 3 independent experiments, with at least 100 cells analyzed in each experiment. Mann-Whitney U test was used for statistical analysis for all comparisons. ** $p < 0.01$ for all panels.

the contacts themselves, rather than distribution within the cell, a limited area was selected in high-magnification images. This approach enabled us to extract three independent areas for measurements and to document more detailed changes in these parameters. Subsequent measurements, based on manual threshold adjustment in the 'Analyze Particles' tool, were conducted to determine number and area of FAs. At least 30 cells from three experiments were examined in each group. No significant differences were observed between the areas of the identical groups selected in the different experiments. The obtained values were summarized separately for each control and experimental group. Subsequently, the corresponding groups of cell contacts were distinguished by the size of the area occupied by a single focal contact. On the basis of the morphometric measurements for each type of the cell culture, the FAs were classified into three categories: immature (area $\leq 2 \mu\text{m}^2$), ma-

ture (area $\sim 2\text{-}6 \mu\text{m}^2$), and supermature (area $\geq 6 \mu\text{m}^2$). Finally, the average percentage of FAs for three experiments was presented as the distribution of the contacts with different areas.

RESULTS

Human subcutaneous fibroblasts were chosen as an optimal cell culture. The objective of this study was to examine the mechanisms of induced differentiation. For this purpose, subcutaneous fibroblasts and dental pulp fibroblasts from healthy donors were used. Expression of the specific markers was subsequently analyzed in both samples after culturing of the treated cells for varying periods.

In the course of experiments conducted with different fibroblast cultures, identification of α -SMA (primary marker of myofibroblasts) revealed that

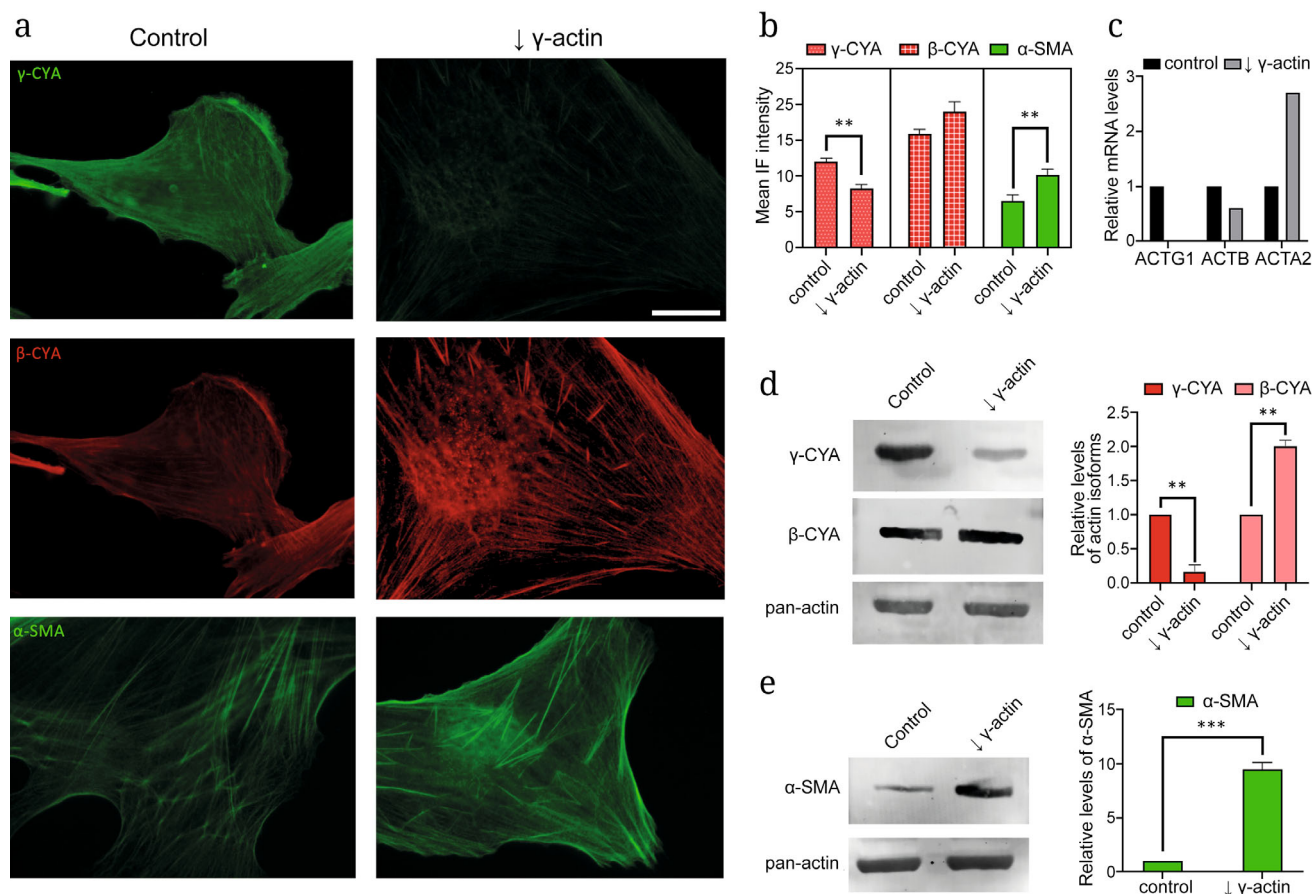


Fig. 2. a) IF staining for γ -CYA, β -CYA, α -SMA in human subcutaneous fibroblasts 9 days after shRNA treatment, scale bar – 25 μ m. b) γ -CYA, β -CYA, and α -SMA fluorescence intensity in subcutaneous fibroblasts 9 days after infection. Graphs show mean \pm SEM. c) RNA profiling data, given in relative units for human subcutaneous fibroblasts 9 days after RNA interference. *ACTA2* – gene of α -smooth muscle actin, *ACTB* – gene of β -cytoplasmic actin, *ACTG1* – gene of γ -cytoplasmic actin. d, e) WB analysis of actin isoforms in human subcutaneous fibroblasts with downregulated γ -CYA. Graphs show relative levels of actin isoforms (mean \pm SEM), the mean was calculated based on a minimum of 3 independent experiments, with at least 100 cells analyzed in each experiment. Mann-Whitney U-test was used for statistical analysis for all comparisons. ** $p < 0.01$, *** $p < 0.001$ for all panels.

the more efficient differentiation was observed in the culture of subcutaneous fibroblasts (Fig. 1a). On the contrary, the same processes occurred at a significantly slower rate in the dental pulp fibroblasts (Fig. 1b). Downregulation of γ -CYA was more effective in the case of subcutaneous fibroblasts, resulting in a higher percentage of the cells with activated myofibroblast phenotype (Fig. 1c).

Furthermore, it was determined that the optimal period for observation of induced differentiation is 9 days, as structural changes in the cytoskeleton and changes in expression of the corresponding actin isoforms were significantly more pronounced than those observed at the day 5 post-infection (Fig. 1d).

However, the use of dental pulp fibroblasts with reduced proliferative activity offers a significant advantage for the detection of specific markers. In particular, organization of some proteins of focal adhesions, such as paxillin, requires long-term contin-

uous cultivation of the cells on the same substrate. Consequently, their highest expression would be observed in the dental pulp fibroblasts at a later point in time.

A decrease of γ -CYA expression was accompanied by an increase of the β -CYA and α -SMA expression. In the course of investigation of fibroblasts with downregulated γ -CYA, it was observed that a change in the amount of one actin isoform was compensated by a reciprocal change in the other. Specifically, a decrease in the level of γ -CYA was accompanied by an increase in the expression of α -SMA and β -CYA in all infected cells (Fig. 2a). Therefore, the overall quantity of actin (pan-actin) remained unaltered. Such compensation was observed at both mRNA and protein levels. However, while γ -CYA was almost completely downregulated at the mRNA level (Fig. 2c), less significant downregulation was observed in the WB analysis (Fig. 2, d, e) and IF staining (Fig. 2b). This suggests

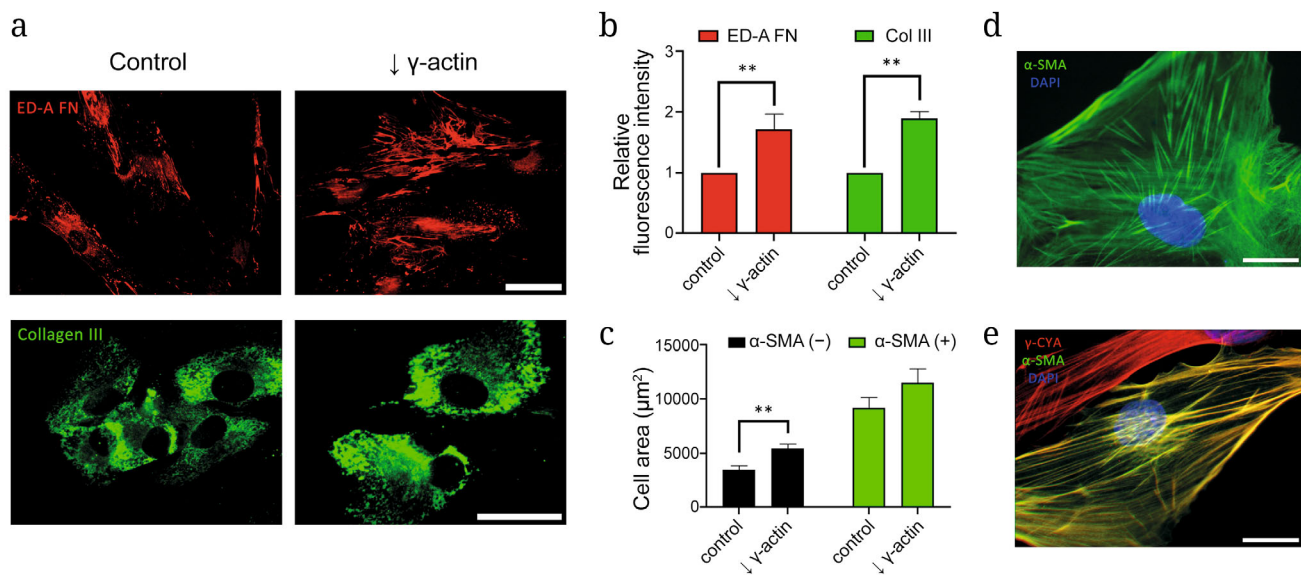


Fig. 3. Upregulation of myofibroblast markers in human subcutaneous fibroblasts after γ -CYA downregulation. a) IF staining for ED-A FN (red, scale bar – 50 μ m) and collagen III (green, scale bar – 25 μ m), control in comparison to shRNA against γ -CYA (9 days after infection). b) ED-A FN and collagen III fluorescence intensity (9 days after infection), presented in arbitrary units. Graphs show mean \pm SEM. c) Changes in the cell area (μ m²) of the fibroblasts in control and in the cells with downregulated γ -CYA (5 days after infection). d) Formation of stress fibers 5 days after γ -CYA downregulation. IF staining for α -SMA (green), DAPI (blue) was used for DNA (nuclear) staining. Scale bar – 25 μ m. e) Formation of a nuclear-associated actin network in the fibroblasts with downregulated γ -CYA (5 days after infection). IF staining for γ -CYA (red) and α -SMA (green), DAPI (blue) was used for DNA (nuclear) staining. Scale bar – 25 μ m. Mann–Whitney U-test was used for statistical analysis for all comparisons. ** $p < 0.01$ for all panels. The mean was calculated based on a minimum of 3 independent experiments, with at least 100 cells analyzed in each experiment.

the existence of a complex post-transcriptional rearrangement in the case of different actin isoforms.

Evidence for effectiveness of the induced differentiation of fibroblasts into myofibroblasts following γ -CYA downregulation. To confirm the presence of induced differentiation, the most commonly used cytoskeletal marker proteins were selected as positive controls, specifically α -SMA and ECM proteins such as ED-A FN, elastin, and collagens of various types.

The measured IF intensity of ED-A FN and type III collagen in the control group and in the fibroblasts with downregulated γ -CYA allowed us to reveal a substantial increase in the expression of these markers in the activated cells (Fig. 3 a and b).

Changes in the fluorescence intensity of elastin in the control and in the culture with downregulated γ -CYA were not statistically significant. The observed decrease in type I collagen in the γ -CYA-depleted cells was contrary to the theoretical expectations, and could probably be associated with the processes related to the timing of cell differentiation in culture (data not shown).

The results of the IF staining assay for paxillin will be discussed in detail in the following section, which is related to maturation of the focal adhesions.

The success of differentiation of fibroblasts into myofibroblasts was further confirmed by the negative

control markers – SMM and desmin. These markers are characteristic of smooth muscle cells and absent in myofibroblasts. In the presence of α -SMA, a common marker for both cell types, there was no staining of SMM and desmin in the fibroblasts with downregulated γ -CYA (data not shown). Morphometric analysis of positive and negative markers of myofibroblasts enabled us to determine the precise direction of the induced differentiation.

Downregulation of γ -CYA expression in human subcutaneous fibroblasts resulted in an increase in the cell area. Differences in the morphology of control fibroblasts and fibroblasts with downregulated γ -CYA were already evident when observed by phase-contrast microscopy (data not shown). Control fibroblasts, particularly those lacking α -SMA, had an elongated shape with long tails (sometimes spindle-shaped) and did not have prominent stress fibers. The fibroblasts with downregulated γ -CYA had a polygonal shape, a significantly larger cell area, and more flattened edges on the surface.

Areas of the cells with downregulated γ -CYA expression were significantly larger than those in the control group (Fig. 3c). This was observed even in the cells that did not have time to develop a prominent actin network after infection with lentiviral constructs due to insufficient differentiation time (Fig. 3c, left).

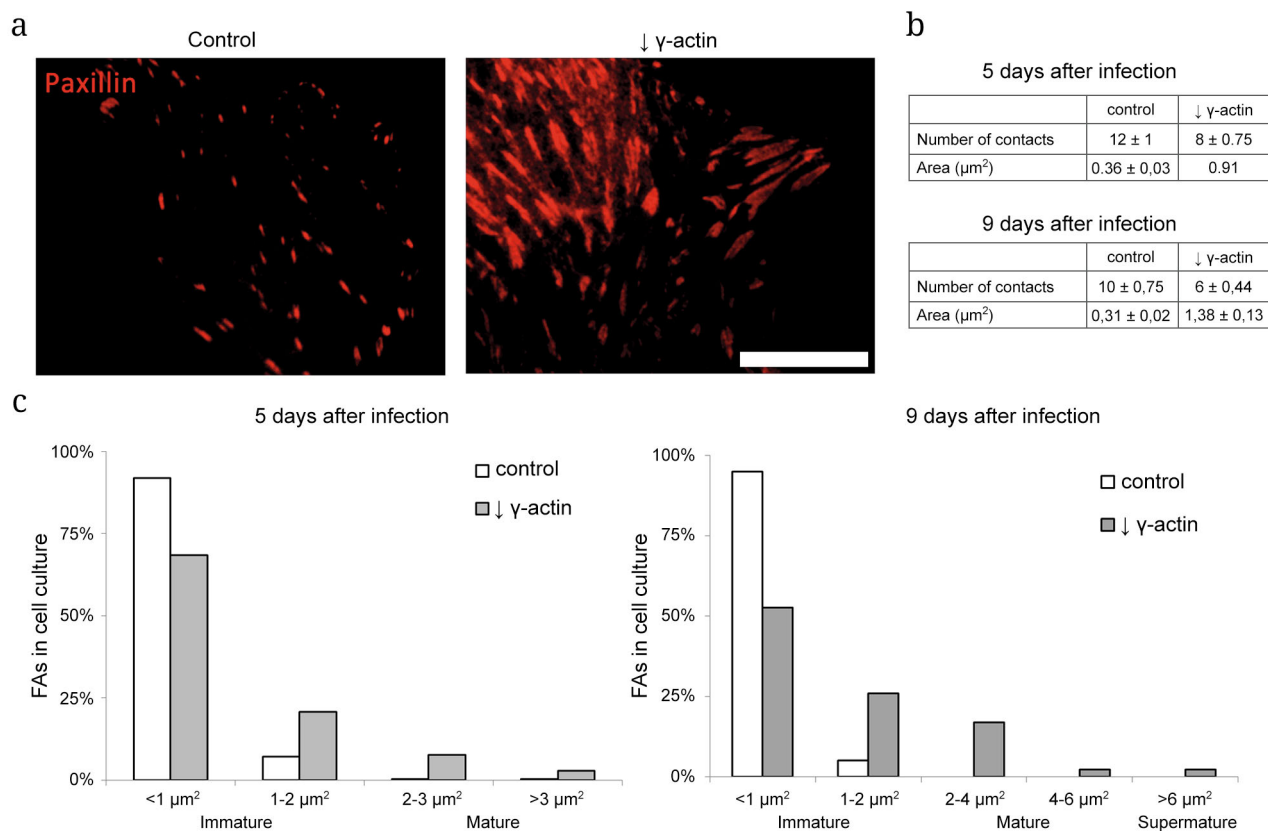


Fig. 4. a) IF staining for paxillin in human subcutaneous fibroblasts 9 days after infection investigated in the control and in the cells with downregulated γ -CYA. Scale bar – 10 μm . b) Dynamics of FAs maturation 5 and 9 days after infection with lentiviral constructs. c) Histograms of distribution of FAs with different areas, 5 and 9 days after infection, control compared to the cells with downregulated γ -CYA. FAs of at least 30 cells were calculated per experiment, based on the data from at least three independent experiments.

It is noteworthy that a certain percentage of α -SMA-positive cells was observed in the control culture, although this was significantly lower than in the γ -CYA-depleted cells (Fig. 3c, right). In order to classify the cells as α -SMA-positive or α -SMA-negative, it was necessary to consider not only the intensity of the corresponding IF staining, but also the structural organization of the actin network. In particular, in the cells with downregulated γ -CYA, formation of the characteristic actin bundles or stress fibers (Fig. 3d) and specific actin network associated with the nucleus or near-nuclear (Fig. 3e) were observed.

Myofibroblastic transition was accompanied by maturation of the focal adhesions. Focal adhesions (FAs), specialized contact sites between the cells and ECM, play an important role in mechanotransduction, a process that stimulates myofibroblast differentiation, which, as we can see from the previous section, occurs better in the fibroblasts with downregulated γ -CYA. To evaluate the dynamics of focal adhesion maturation, IF staining for paxillin was used (Fig. 4a). Estimates of the number of FAs per 100 μm^2 area and their area measurements in the control and γ -CYA downregulated cells are presented in the Tables (Fig. 4b).

To evaluate the degree of maturation at different stages, cell cultures were observed following infection with lentiviral constructs for 5 and 9 days (Fig. 4b).

The majority of the FAs observed in the cells from the control cultures were immature, although a significant number of such FAs were also present in the cells with downregulated γ -CYA. The number of mature focal contacts was higher in the cells with downregulated γ -CYA, although they were also present in relatively small numbers in the control cells. Formation of the supermature contacts was observed exclusively in the cells with downregulated γ -CYA (Fig. 4c).

In conclusion, the results of morphometric analysis demonstrate that differentiation of fibroblasts into myofibroblasts was accompanied by the process of maturation or fusion of FAs. This is evidenced by a decrease in the number of individual contacts, accompanied by an increase in their area.

DISCUSSION

Actin is a highly conserved protein and the greatest divergences are observed when the muscle and

cytoplasmic isoforms are compared. Amino acid residues important for formation of the fibrillar actin are mostly identical, and the major differences in the amino acid composition are concentrated in the N-terminal region, outside of the subdomain 1. In particular, β -CYA and γ -CYA differ by only four amino acid residues in this sub-region [14, 15]. Despite the fact that actin isoforms exhibit a high degree of similarity in terms of their amino acid sequences, there are nevertheless notable differences in their localization and functional roles within the cell. β -CYA is predominantly present in stress fibers, whereas γ -CYA is detected mainly as an apical dense network [2]. Some studies have indicated that minor variations in the N-terminal sequence of β -CYA and γ -CYA may affect their affinity for actin-binding proteins (ABPs) [16].

While the degree of difference between β -CYA and γ -CYA at the amino acid level is only 1%, it exceeds 11% for the corresponding mRNAs. In addition, the β -CYA mRNA is initially synthesized at a rate six times higher than that of γ -CYA. However, no such significant difference is observed at the protein level, apparently indicating that the majority of β -CYA transcripts are repressed and stored for potential rapid translation of the corresponding protein and dynamic rearrangement of the cytoskeleton [1]. The observed discrepancies in the mRNA and protein levels could be explained by the fact that β -CYA is a more dynamic isoform that is critically required by the cell for cytoskeletal rearrangement. Taking into account the fact that we used adult donor fibroblasts, degradation of the already translated γ -CYA protein was slower and the effect of silencing was significantly less at the protein level, despite the expected drastic decrease in the mRNA level [1, 17].

Myofibroblasts are of heterogeneous origin, which means that they are derived from the different types of precursors via appropriate processes, with fibroblast differentiation representing only one potential pathway [18]. However, properties of the fibroblasts themselves could vary depending on their localization. The more efficient differentiation of the subcutaneous fibroblasts has been observed for a reason: this cell type is inherently richer in the relevant markers, as their localization implies greater dynamics and susceptibility to mechanotransduction – a phenomenon that determines the dependence of myofibroblast differentiation on the changes in mechanical stress caused by both exogenous and endogenous factors. This applies not only to the organization of the fibroblast cytoskeleton, but also to the synthesis of ECM proteins [19]. In particular, these features are directly reflected in the organization of the cell–cell contacts, which include some of the markers we have investigated. Despite the established role of ED-A FN in myofibroblast differentiation, the mechanism underlying this

process remains unclear. However, it has been suggested that ED-A FN could interact with the fibroblast cell surface receptors and participate in the TGF β 1-mediated signaling pathway. Indeed, the data obtained from RNA profiling (data not shown) indicate an increase in the TGFB2 and corresponding TGFBR2 (TGF β receptor 2) transcripts. At the same time, the level of TGFBR3 (TGF β receptor 3) transcript is reduced by approximately 20%, suggesting that co-reception may be redundant under the new differentiation conditions. Accumulation of ED-A FN is frequently observed in the cases of fibrosis. Unique expression of ED-A FN and its key role in the development of the myofibroblast phenotype makes this protein an attractive target for anti-fibrotic therapy [20, 21]. Morphometric changes observed in this study, including changes in the cell area and shape, are consistent with the previously published data [22, 23]. We suggest that downregulation of γ -CYA induces alterations in the expression of ECM proteins, increases microenvironment stiffness, and thus stimulates the formation of supermature FAs, which are associated with mechanotransduction. As a result, we observe transition of fibroblasts to the protomyofibroblast state [24, 25].

The observed involvement of γ -CYA in the phenotypic switching could be attributed to its normal physiological functions in the cytoskeletal rearrangements of the developing cells. Previously, it has been demonstrated that suppression of the Rho-kinase-dependent cell migration is associated with a decrease in γ -CYA expression during neuroblastoma differentiation [26]. In addition, γ -CYA inhibits myofibroblastic cell trans-differentiation through two complementary mechanisms: by regulating the G-/F-actin ratio and by binding to the myocardin-related transcription/serum response factor (MRTF/SRF) complex. Importantly, it is γ -CYA that preferentially binds to MRTF-A and SRF, resulting in the appropriate transcription program being initiated upon depletion of this isoform [27].

CONCLUSION

In the course of our investigation, we established experimental conditions for the induced differentiation of fibroblasts into myofibroblasts through the downregulation of γ -CYA expression (Fig. 5). On the basis of the morphometric data and of the marker expression profile, human subcutaneous fibroblasts were identified as an optimal cell culture for our research. A decrease in the γ -CYA expression was accompanied by a compensatory increase in the expression of other actin isoforms. Changes were revealed at the mRNA level, at the protein level, and at the level of immunofluorescence signal. The fibroblasts with fully or partially downregulated γ -CYA had an increased

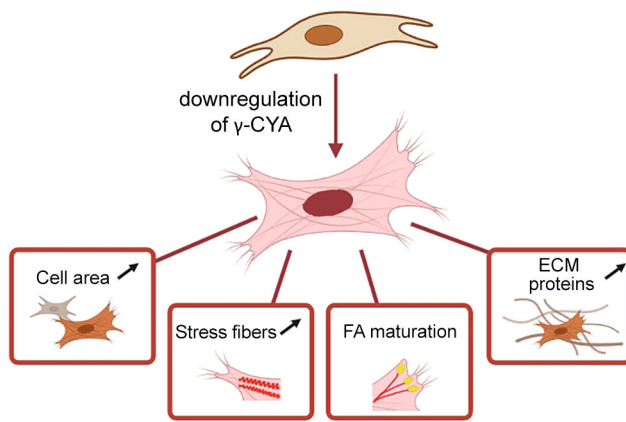


Fig. 5. Scheme illustrating the features of the fibroblast-to-myofibroblast differentiation induced by γ -CYA downregulation.

area, distinct stress fibers, mature and supermature FAs, which are typical of the myofibroblast phenotype. Efficiency of the induced differentiation of fibroblasts into myofibroblasts was evaluated through the use of positive differentiation markers, including α -SMA, type III collagen, and ED-A FN. The IF staining for negative control markers, such as SMM and desmin, was used to further elucidate the differentiation pathway and exclude the induction of similar cell types.

Contributions. Conceptualization, V.D.; methodology, V.D.; software, Yu.L.; validation, G.S., V.D. and P.K.; formal analysis, S.B. and P.K.; investigation, N.K., Yu. L. and V.D.; resources, I.E. and P.K.; data curation P.K.; writing – original draft preparation, Yu. L.; writing – review and editing, V.D. and G.S.; visualization, N.K., Yu.L. and V.D.; supervision, P.K.; project administration, P.K.; funding acquisition, P.K. All authors have read and agreed to the published version of the manuscript.

Funding. This work was financially supported by the Russian Science Foundation (grant no. 23-15-00433), <https://rscf.ru/en/project/23-15-00433/>.

Ethics approval and consent to participate. This work does not contain any studies involving human and animal subjects.

Conflict of interest. The authors of this work declare that they have no conflicts of interest.

REFERENCES

1. Patrinostru, X., O'Rourke, A. R., Chamberlain, C. M., Moriarity, B. S., Perrin, B. J., and Ervasti, J. M. (2017) Relative importance of β cyto-and γ cyto-actin in primary mouse embryonic fibroblasts, *Mol. Biol. Cell*, **28**, 771-782, <https://doi.org/10.1091/mbc.E16-07-0503>.
2. Dugina, V., Zwaenepoel, I., Gabbiani, G., Clément, S., and Chaponnier, C. (2009) β - and γ -cytoplasmic actins

display distinct distribution and functional diversity, *J. Cell Sci.*, **122**, 2980-2988, <https://doi.org/10.1242/jcs.041970>.

3. Simiczjzew, A., Pietraszek Gremplewicz, K., Mazur, A. J., and Nowak, D. (2017) Are non-muscle actin isoforms functionally equivalent, *Histol. Histopathol.*, **32**, 1125-1139, <https://doi.org/10.14670/HH-11-896>.
4. Bunnell, T. M., Burbach, B. J., Shimizu, Y., and Ervasti, J. M. (2011) β -Actin specifically controls cell growth, migration, and the G-actin pool, *Mol. Biol. Cell*, **22**, 4047-4058, <https://doi.org/10.1091/mbc.E11-06-0582>.
5. Hinz, B., Dugina, V., Ballestrem, C., Wehrle-Haller, B., and Chaponnier, C. (2003) α -Smooth muscle actin is crucial for focal adhesion maturation in myofibroblasts, *Mol. Biol. Cell*, **14**, 2508-2519, <https://doi.org/10.1091/mbc.e02-11-0729>.
6. Otranto, M., Sarrazy, V., Bonté, F., Hinz, B., Gabbiani, G., and Desmouliere, A. (2012) The role of the myofibroblast in tumor stroma remodeling, *Cell Adhes. Migrat.*, **6**, 203-219, <https://doi.org/10.4161/cam.20377>.
7. Tripathi, M., Billet, S., and Bhowmick, N. A. (2012) Understanding the role of stromal fibroblasts in cancer progression, *Cell Adhes. Migrat.*, **6**, 231-235, <https://doi.org/10.4161/cam.20419>.
8. Gabbiani, G. (2003) The myofibroblast in wound healing and fibrocontractive diseases, *J. Pathol.*, **200**, 500-503, <https://doi.org/10.1002/path.1427>.
9. Aujla, P. K., and Kassiri, Z. (2021) Diverse origins and activation of fibroblasts in cardiac fibrosis, *Cell Signall.*, **78**, 109869, <https://doi.org/10.1016/j.cellsig.2020.109869>.
10. Arnoldi, R., Chaponnier, C., Gabbiani, G., and Hinz, B. (2012) Chapter 88 – Heterogeneity of smooth muscle, In *Muscle* (Hill, J. A. and Olson, E. N., eds) *Academic Press*, **2**, 1183-1195, <https://doi.org/10.1016/B978-0-12-381510-1.00088-0>.
11. Younesi, F. S., Son, D. O., Firmino, J., and Hinz, B. (2021) Myofibroblast markers and microscopy detection methods in cell culture and histology, *Methods Mol. Biol.*, **2299**, 17-47, https://doi.org/10.1007/978-1-0716-1382-5_3.
12. Dugina, V., Khromova, N., Rybko, V., Blizniukov, O., Shagieva, G., Chaponnier, C., Kopnin, B., and Kopnin, P. (2015) Tumor promotion by γ and suppression by β non-muscle actin isoforms, *Oncotarget*, **6**, 14556-14571, <https://doi.org/10.18632/oncotarget.3989>.
13. Dugina, V., Shagieva, G., Khromova, N., and Kopnin, P. (2018) Divergent impact of actin isoforms on cell cycle regulation, *Cell Cycle*, **17**, 2610-2621, <https://doi.org/10.1080/15384101.2018.1553337>.
14. Ampe, C., and Van Troys, M. (2017) Mammalian actins: isoform-specific functions and diseases, *Handb. Exp. Pharmacol.*, **235**, 1-37, https://doi.org/10.1007/164_2016_43.

15. Arora, A. S., Huang, H. L., Singh, R., Narui, Y., Suchenko, A., Hatano, T., Heissler, S. M., Balasubramanian, M. K., and Chinthalapudi, K. (2023) Structural insights into actin isoforms, *Elife*, **12**, e82015, <https://doi.org/10.7554/eLife.82015>.
16. Heissler, S. M., and Chinthalapudi, K. (2024) Structural and functional mechanisms of actin isoforms, *FEBS J.*, **81**, 263, <https://doi.org/10.1111/febs.17153>.
17. Bergeron, S. E., Zhu, M., Thiem, S. M., Friderici, K. H., and Rubenstein, P. A. (2010) Ion-dependent polymerization differences between mammalian β - and γ -non-muscle actin isoforms, *J. Biol. Chem.*, **285**, 16087-16095, <https://doi.org/10.1074/jbc.M110.110130>.
18. Hinz, B., Phan, S. H., Thannickal, V. J., Galli, A., Bochaton-Piallat, M. L., and Gabbiani, G. (2007) The myofibroblast: one function, multiple origins, *Am. J. Pathol.*, **170**, 1807-1816, <https://doi.org/10.2353/ajpath.2007.070112>.
19. D'Ardenne, A. J., Burns, J., Sykes, B. C., and Kirkpatrick, P. (1983) Comparative distribution of fibronectin and type III collagen in normal human tissues, *J. Pathol.*, **141**, 55-69, <https://doi.org/10.1002/path.1711410107>.
20. Muro, A. F., Moretti, F. A., Moore, B. B., Yan, M., Atrasz, R. G., Wilke, C. A., Flaherty, K. R., Martinez, F. J., Tsui, J. L., Sheppard, D., Baralle, F. E., Toews, G. B., and White, E. S. (2008) An essential role for fibronectin extra type III domain A in pulmonary fibrosis, *Am. J. Respir. Crit. Care Med.*, **177**, 638-645, <https://doi.org/10.1164/rccm.200708-1291OC>.
21. Tai, Y., Woods, E. L., Dally, J., Kong, D., Steadman, R., Moseley, R., and Midgley, A. C. (2021) Myofibroblasts: function, formation, and scope of molecular therapies for skin fibrosis, *Biomolecules*, **11**, 1095, <https://doi.org/10.3390/biom11081095>.
22. Ragoowansi, R., Khan, U., Brown, R. A., and McGrouther, D. A. (2003) Differences in morphology, cytoskeletal architecture and protease production between zone II tendon and synovial fibroblasts *in vitro*, *J. Hand Surg.*, **28**, 465-470, [https://doi.org/10.1016/s0266-7681\(03\)00140-2](https://doi.org/10.1016/s0266-7681(03)00140-2).
23. Dugina, V., Alexandrova, A., Chaponnier, C., Vasiliev, J., and Gabbiani, G. (1998) Rat fibroblasts cultured from various organs exhibit differences in α -smooth muscle actin expression, cytoskeletal pattern, and adhesive structure organization, *Exp. Cell Res.*, **238**, 481-490, <https://doi.org/10.1006/excr.1997.3868>.
24. Goffin, J. M., Pittet, P., Csucs, G., Lussi, J. W., Meister, J. J., and Hinz, B. (2006) Focal adhesion size controls tension-dependent recruitment of α -smooth muscle actin to stress fibers, *J. Cell Biol.*, **172**, 259-268, <https://doi.org/10.1083/jcb.200506179>.
25. Younesi, F. S., and Hinz, B. (2024) The myofibroblast fate of therapeutic mesenchymal stromal cells: regeneration, repair, or despair? *Int. J. Mol. Sci.*, **25**, 8712, <https://doi.org/10.3390/ijms25168712>.
26. Shum, M. S., Pasquier, E., Po'uha, S. T., O'Neill, G. M., Chaponnier, C., Gunning, P. W., and Kavallaris, M. (2011) γ -Actin regulates cell migration and modulates the ROCK signaling pathway, *FASEB J.*, **25**, 4423-4433, <https://doi.org/10.1096/fj.11-185447>.
27. Lechuga, S., Baranwal, S., Li, C., Naydenov, N. G., Kuemmerle, J. F., Dugina, V., Chaponnier, C., and Ivanov, A. I. (2014) Loss of γ -cytoplasmic actin triggers myofibroblast transition of human epithelial cells, *Mol. Biol. Cell*, **25**, 3133-3146, <https://doi.org/10.1091/mbc.E14-03-0815>.

Publisher's Note. Pleiades Publishing remains neutral with regard to jurisdictional claims in published maps and institutional affiliations. AI tools may have been used in the translation or editing of this article.